We are IntechOpen,
the world's leading publisher of Open Access books
Built by scientists, for scientists

6,900
Open access books available

186,000
International authors and editors

200M
Downloads

Our authors are among the

154
Countries delivered to

TOP 1%
most cited scientists

12.2%
Contributors from top 500 universities

BOOK CITATION INDEX
CLARIVATE ANALYTICS
INDEXED

WEB OF SCIENCE™

Selection of our books indexed in the Book Citation Index
in Web of Science™ Core Collection (BKCI)

Interested in publishing with us?
Contact book.department@intechopen.com

Discrete Wavelet Transforms for Synchronization of Power Converters Connected to Electrical Grids

Alberto Pigazo and Víctor M. Moreno
University of Cantabria
Spain

1. Introduction

Electronic power converters connected to electrical grids allow industrial processes, traction applications and home appliances to be improved by controlling the energy flow depending on the operation conditions of both the electrical load and the grid. This is the case of variable frequency drives, which can be found in pump drives or ship propulsion systems (Bose, 2009) maintaining the electrical machine in the required operation state while ensuring a proper current consumption from the electrical grid. Recent researching and developing efforts on grid-connected power converters are due to the integration of renewable energy sources in electrical grids, which requires the implementation of new functionalities, such as grid support, while maintaining reduced current distortion levels and an optimal power extraction from the renewable energy source (Carrasco et al., 2006; Liserre et al., 2010).

In the most general case, a grid-connected power converter consists of power and control stages which ensures the appropriate energy management (Erickson & Maksimovic, 2001; Mohan et al., 2003). In the first one, electronic power devices, such as power diodes, thyristors, insulated gate bipolar transistors (IGBTs) or MOS-controlled thyristors (MCTs), and passive elements (inductances and capacitors) are found. The switching state of the power devices allows the voltage or/and current across the passive components to be controlled. Resistive behaviors must be minimized in order to avoid conduction power losses. The second stage, in case of controlled semiconductor devices, consists of a signal conditioning system and the required hardware for implementation of the converter controller (Bose, 2006).

Recent advances in field programmable gate arrays (FPGAs) and digital signal processors (DSPs) allow the complexity and functionalities of the controllers employed in power converters to be increased and improved (Bueno et al., 2009). In grid-connected power converters these functionalities include, in most cases, the synchronization with the electrical grid, the evaluation of the reference current amplitude at the grid-side and current control (Kazmierkowski et al., 2002). The amplitude and phase of the grid-side current depends on the reference current evaluation and the synchronization subsystems while the current controller ensures that the current waveform matches the reference one. The implementation of these subsystems depends on the application characteristics. Other functionalities, such as grid support (Ullah et al., 2009) or detection of the islanding condition (De Mango, Liserre & D'Aquila, 2006; De Mango, Liserre, D'Aquila & Pigazo, 2006), can be added if it is required.

These controller functionalities can be implemented by applying diverse approaches, such as digital signal processing techniques, i.e. Fourier Transforms (McGrath et al., 2005), Kalman

Filters (Moreno et al., 2007) or Discrete Wavelet Transforms (DWTs) (Pigazo et al., 2009). Frequency and time localization of wavelet analysis allow the performance of controllers in grid-connected power converters to be improved. This is the case of active power filters, where the compensation reference current can be evaluated by means of DWT (Driesen & Belmans, 2002), modulation techniques in controlled rectifiers (Saleh & Rahman, 2009) or the controller design process using averaging models of power converters (Gandelli et al., 2001).

This book chapter proposes to take advantage of DWTs' properties in order to improve the synchronization subsystem of controllers in grid-connected power converters. After a review of the state of art in wavelet analysis applied to power electronics, the main characteristics of controllers in grid-connected power converters are presented as well as the new approach for synchronization purposes. Results validating the proposal, considering diverse operation conditions, are shown.

2. Wavelet analysis applied to power converters

The wavelet analysis has been mainly applied to signal analysis and processing (i.e. identification and classification) in electrical power systems (voltage and current) during the last twenty years (Ribeiro, 1994; Robertson et al., 1994). The wavelet analysis was firstly applied to power system protection, power quality measurement, detection of power system transients, partial discharges, forecasting of electrical loads due to its its capability for fast and accurate identification of transients (Castro & Diaz, 2002). In recent years this signal processing technique has been also applied in order to control power electronic converters, such as dc-dc, inverters, rectifiers, active power filters and unified power quality conditioners (UPQCs). This chapter section shows some of these applications both to power systems and, more specifically, power converters.

2.1 Wavelet analysis in power systems

The power system protection can be improved by applying the wavelet analysis to activate the relays in case of power system transients. Time resolution capability of the wavelet analysis is employed in (Chaari et al., 1996) for detection of earth faults in case of a 20 kV resonant grounded network. High impedance faults identification and protection of transformers and generators by means of wavelets are also shown in (Solanki et al., 2001) and (Eren & Devaney, 2001) respectively. In this last case, the frequency resolution of wavelets allows the changes of the power signals' spectra to be measured in order to detect the degradation of the insulation and identify internal and external faults. Wavelets have been also employed for modeling of electrical machines in wind turbines and detection of turn-to-turn rotor faults (Dinkhauser & Fuchs, 2008).

The evaluation of the electrical power quality (PQ) can take advantage of wavelet analysis for detection and measurement of interferences, impulses, notches, glitches, interruptions, harmonics, flicker and other disturbances. In case of harmonic currents/voltages and voltage flicker the multiresolution analysis (MRA) using wavelet filter banks (Pham & Wong, 1999; Pham et al., 2000) and continuous wavelet transforms (Zhen et al., 2000) can be applied. The propagation of power system transients can be also analyzed by means of wavelets (Heydt & Galli, 1997; Wilkinson & Cox, 1996). The characteristics of partial discharges (short duration, high frequency and low amplitude) make it difficult to detect. Wavelet analysis allows partial discharges to be detected due to its time resolution, as it is shown in (Shim et al., 2000) in case of transformer windings and cables.

The efficient management of electrical power system requires a proper forecasting of electrical loads. The combination of wavelets and neural networks in (Huang & Yang, 2001; Yao et al., 2000) allows it by considering the current waveforms as a linear combination of different frequencies. The wavelet analysis can also be applied for measurement of the electrical active/reactive power and the root mean square (rms) value of line voltages and currents on a frequency band basis (Hamid & Kawasaki, 2001).

2.2 Wavelet analysis in controllers for power converters

Wavelets have been recently applied in power converters used in diverse applications. The covered functionalities include modeling of the power converter, its control and supervision tasks.

In order to obtain a more flexible model of a dc/dc power converter, wavelets are applied in (Ponci et al., 2009) for detection of the operation mode of the power converter, consisting on an extension of conventional analysis techniques based on state-space averaging. A model of a dc/ac converter based on wavelets is obtained in (Gandelli et al., 2002) in order to perform a detailed analysis and the optimization of the power converter.

Wavelet-based controllers have been also proposed in literature in order to improve the performance of the power converter. This is the case of (Hsu et al., 2008), where a wavelet-based neural network is employed in order to minimize the impact of input voltage and load resistance variations on a dc/dc converter. In (Saleh & Rahman, 2009) wavelets allow a new switching strategy to be developed in order to reduce the harmonic content of the output voltage in a ac/dc converter maintaining unity power factor. A three-phase induction generator (IG) system for stand-alone power systems is controlled by means of one ac/dc plus one dc/ac converter and applying a recurrent wavelet neural network (RWNN) controller with improved particle swarm optimization (IPSO) (Teng et al., 2009). The controllers in dc/ac converters can be optimized by applying wavelets, this is the case of (Mercorelli et al., 2004), where it is employed for optimization of the applied model predictive controller. The wavelet analysis is applied in (González et al., 2008) in order to evaluate the performance of the employed modulation technique, including the spectrum of the converter output voltage and its ripple. Controllers in multilevel converters can also take advantage of wavelets, as it is shown in (Iwaszkiewicz & Perz, 2007), in order to ensure a better and faster adaptation of their output voltage waveforms to sine waveforms and reduce the harmonic distortion of the output voltage at relatively low switching frequencies. High-level control functionalities, such as islanding detection or source impedance measurement, required in distributed generation systems connected to electrical grids can also obtain benefits from the wavelet analysis. The high frequency bands of voltage and current waveforms are evaluated in (Pigazo et al., 2009; 2007) in order to detect the islanding condition. The power system impedance can be measured in real-time by injecting a controlled disturbance into the electrical grid, the wavelet analysis allows an fast detection of faults (Sumner et al., 2006).The wavelets can be also applied for characterization of power converters' performance. In (Knezevic et al., 2000) the wavelet analysis is applied for measurement of transients caused by ac/dc converters.

3. Controllers in grid-connected power converters

The general structure of a single-phase grid-connected power converter, including both power and control stages, is shown in Fig. 1. The power stage of the dc/ac converter consists of an IGBT full-bridge with diodes, which synthesizes a low frequency ac voltage by changing the IGBTs' switching states, the gate circuit, which applies the required gate signals in order to

switch on and off the controlled power devices, an LCL-filter, employed as a second-order low pass filtering stage which allows the high frequency ripple of the full-bridge output voltage to be filtered out and a dc-side filtering stage, which can be implemented by means of one shunt capacitor (first order) or a series inductance plus a shunt capacitor (second order).
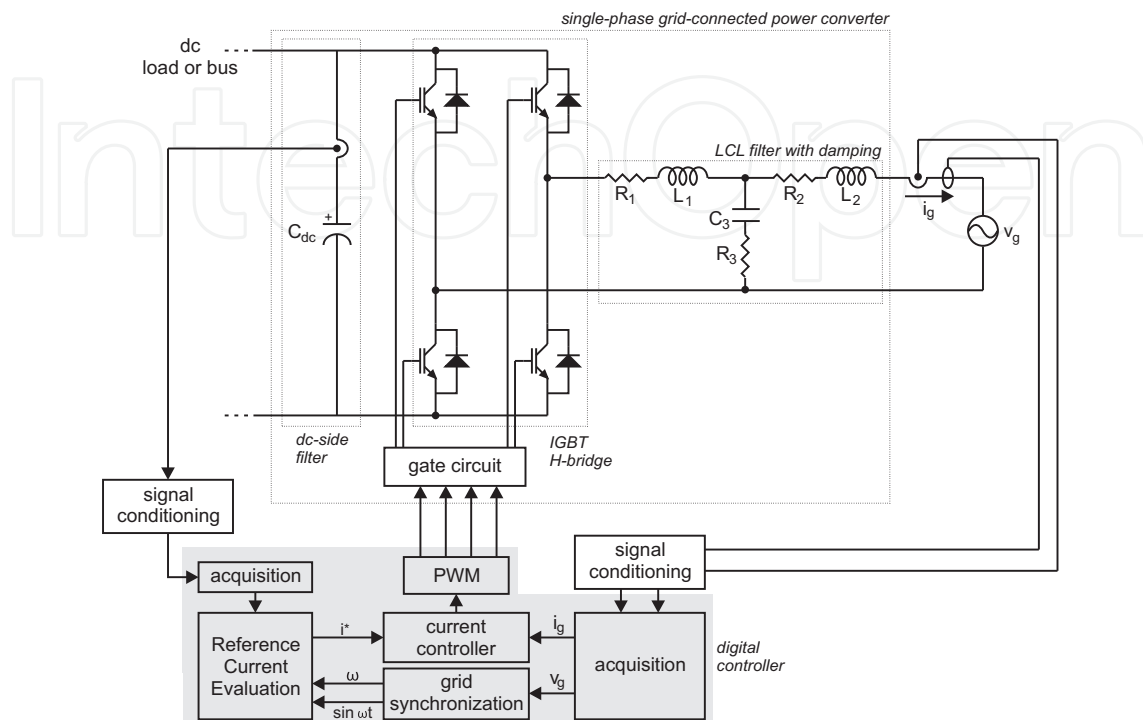

Fig. 1. Three-phases three-wires grid connected dc/ac converter.

Depending on the application characteristics, the converter controller functionalities are implemented using analog or digital circuitries and, in the second case, FPGAs, DPSs and microcontrollers (μCs) allow more flexible and complex controllers to be designed and implemented (Bueno et al., 2008; Koizumi et al., 2006; Kojabadi et al., 2006). In case of grid-connected power converters, both inverters and controlled rectifiers switching at relatively high frequencies (around 10 kHz), the main functionalities that must be implemented are grid synchronization, evaluation of the reference for current injection/consumption, grid side current control and pulse width modulation (PWM) (Kazmierkowski et al., 2002). The grid synchronization block must generate, at least, a reference signal $\sin \omega t$ which must track properly the fundamental component of the grid voltage v_g. Depending on the application, i.e. distributed generation systems, the grid frequency must be also measured in order to implement load sharing algorithms (Guerrero et al., 2004). The evaluation of the instantaneous values of the reference current i^* is required in order to determine the proper current which must flow from/to the electrical grid i_g. The implementation of this functionality depends on the application and, hence, on the implemented high level control functionalities such as reactive power requirements, harmonic control, tolerance to grid disturbances or the maintenance of the dc-bus voltage. The obtained values of i^* are applied to a current controller. This block must ensure that the grid side current i_g matches the reference ones i^*. Diverse approaches, such as hysteresis (Ho et al., 2009), deadbeat (Mohamed & El-Saadany, 2008), proportional-integral (PI) controllers (Dannehl et al., 2010), resonant controllers (Liserre et al., 2006), repetitive controllers (Weiss et al., 2004) or inner model controllers (Gabe et al., 2009), can be found in literature for this purpose.

Finally, the control action must be applied to the gate circuitry of the H-bridge, where square signal waveforms with variable width are required. In order to obtain these variable switching patterns, diverse approaches can be also found. A detailed description of these techniques is available in (Holmes & Lipo, 2003)

4. Synchronization subsystem in grid-connected power converters

Main approaches for synchronization of the power converter to the electrical grid are zero crossing detection (Vainio & Ovaska, 1995; Valiviita, 1999) and phase locked loops (PLLs) (El-Amawy & Mirbod, 1988; Freijedo et al., 2009). While the first one can be easily implemented by means of analog circuitry, power system disturbances such as partial discharges can result on synchronization problems and an erroneous reference current i^*. Due to this fact, the second approach and other based on digital signal processing techniques, i.e. DFT (McGrath et al., 2005) and Kalman filter (Moreno et al., 2007), are preferred. A common approach for implementation of PLLs includes a phase detection (PD) block, a low-pass filtering stage and a voltage controlled oscillator (VCO). By applying the PD block, the input signal v_g is shifted in the frequency domain to low frequency while other frequency components of the input signal are shifted to higher frequencies. The obtained signal is applied to a low-pass filtering stage for filtering out frequency components of the input signal which must not be tracked. Once filtered out, the obtained signal is proportional to the phase error of the input signal v_g and the signal which is generated by the VCO and applied to PD block. Due to the closed loop structure, and depending on the characteristics of the input signal, the PD block and the low-pass filtering stage, the VCO will adjust the relative phase and frequency of the generated signal in order to match the frequency component of v_g to be tracked.

Diverse approaches have been proposed in the literature in order to implement the functional blocks in the previous paragraph but one of the most applied ones in case of grid-connected power converters is based on the Park Transformation. Its general structure for the synchronization of a single-phase grid-connected power converter is shown in Fig. 2. The grid voltage is measured, digitized and applied to the software PLL by means of the input port V_g. This signal is employed to generate a virtual quadrature component, denoted as β, which allows the grid voltage, considered as α, to be represented as a phasor on a stationary complex reference frame (Clarke Transformation), obtaining $\alpha\beta$ components of this single-phase voltage signal. The obtained instantaneous values of this voltage phasor are transformed again by applying the Park Transformation, which carries out a frequency shift of the fundamental frequency tracked by the software PLL. This allows dq components of the voltage phasor, obtained in a rotating reference frame, to be generated. Once the software PLL is tracking the fundamental frequency properly (in phase), the q component of this transformation should be equal to zero and, hence, the instantaneous phase generated by the software PLL should be properly controlled. This is done by the *Controller* block. The impact of possible amplitude variations, i.e. due to voltage sags, can be prevented by means of a normalization block which generates dq components in the range [-1,1]. The *Controller* generates, as a result of its operation and once the software PLL is operating properly, a measure of the grid frequency. The instantaneous phase can be obtained by means of a discrete integrator and, then, a sinusoidal output signal with unity amplitude and in-phase with the grid voltage signal can be generated by applying *sin* and *cos* functions to the measured instantaneous phase. These trigonometric functions are required by the Park Transformation in order to generate the dq components.
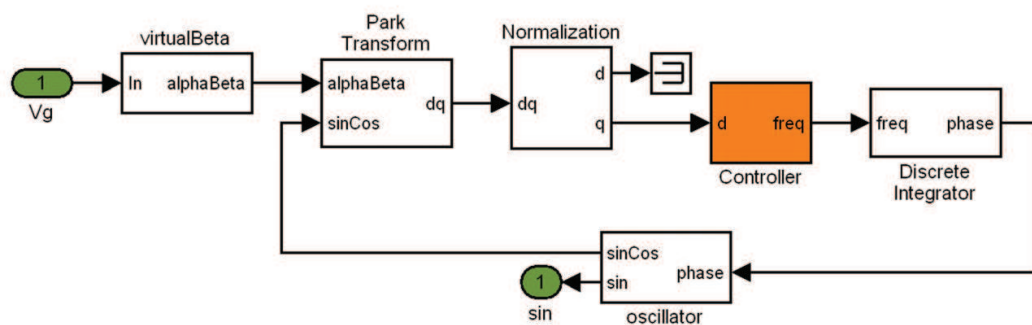
Fig. 2. Structure of software PLL for a single-phase grid-connected power converter.

4.1 Proposed synchronization subsystem

The *Controller* block of the software PLL is commonly implemented as a PI controller or, more generally, as a first order or second order low pass filter, however, recent researching works on DWTs for control applications suggest that the performance of PI controllers can be improved by using DWTs (Parvez & Gao, 2005). The proposed software PLL substitutes the PI controller by a DWT implemented using filter banks. The inner structure of the *Controller* in case of the proposed software PLL is shown in Fig. 3. As it can be seen, it consists of one *Buffer*, where 2^L samples of the input are buffered to be analyzed and L is the number of decomposition levels, the *Dyadic Analysis Filter Bank* from the Signal Processing Blockset in MatLab/Simulink, which generates an output vector containing the output at each sub-band. Then, the loop gains, contained in the *Constant Diagonal Matrix Block* and needed to adjust the response of the proposed software PLL, are applied. Finally, the *Controller* output signal is obtained by adding the current output of the previous stage at each sub-band.
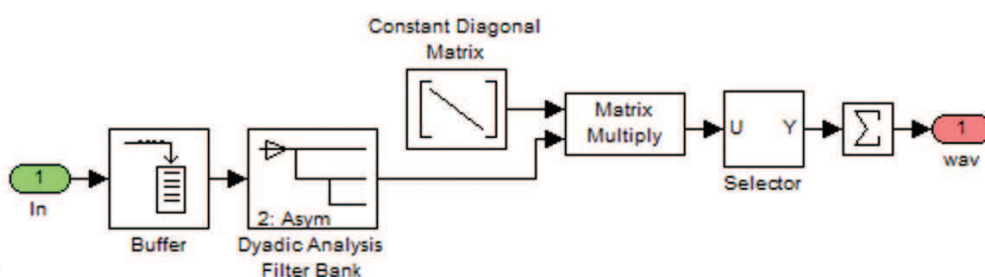

Fig. 3. Controller block in the wavelet PLL (WPLL).

5. Simulation results

In order to analyze the performance of the proposed synchronization block diverse simulation tests have been carried out. After the selection of the most suitable mother wavelet considering diverse decomposition levels and operation conditions, the proposed synchronization system is employed in order to control a dc machine by means of a grid connected controlled rectifier. The applied tests include step amplitude variations of the voltage grid from $23\sqrt{2}$ V to $230\sqrt{2}$ V and step frequency variations from 47.5 Hz to 52.5 Hz, in both cases including a 7% 5th voltage harmonic. The employed sampling frequency is 6.4 kHz.
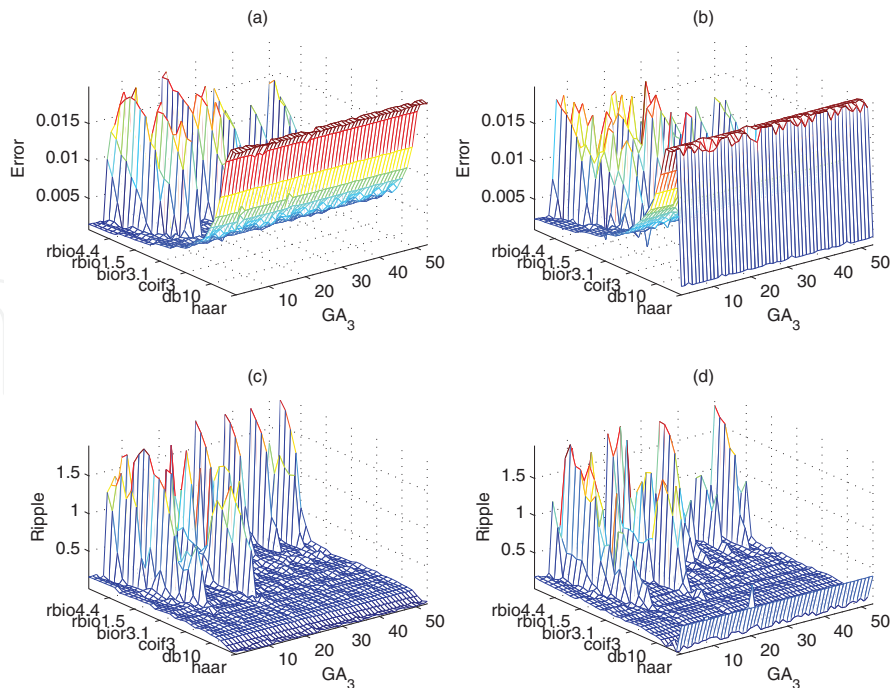
Fig. 4. L=3. a) Magnitude of the WPLL average error after the voltage amplitude step, b) magnitude of the WPLL average error after the fundamental grid frequency step, c) ripple of the WPLL error after the voltage amplitude step and d) ripple of the WPLL error after the voltage amplitude step.

5.1 Selection of the mother wavelet

The selection of the most suitable mother wavelet has been carried out considering decomposition levels (L) in the range $[3, 6]$. At each decomposition level, diverse values of the WPLL loop gains have been applied under the operation conditions described previously. The obtained results, the average error magnitude of the WPLL and the ripple of this error, have been measured $0.5 \, s$ after each transient in order to compare the performance of each mother wavelet. Figs. 4, 5, 6 and 7 show the obtained results for L in $[3, 6]$.

From Fig. 4, the best results at $L = 3$ are obtained by applying a *Daubechies 7* mother wavelet with a loop gain at the lowest frequency sub-band $GA_3 = 39$. In this case, the cumulative measured average error of the WPLL falls to $1.1 \cdot 10^{-3} \, V$ after the first transient, which reaches $5.2 \cdot 10^{-3} \, V$ after the frequency step. The error ripple measured after the grid voltage transients are $0.23 \, V$ and $0.16 \, V$. The worst results are obtained in case of *Daubechies 4* at GA_3, reaching cumulative average errors of $2.0 \cdot 10^{-2} \, V$ after both grid voltage transients. In case of the measured error ripple, it decreases up to $5.4 \cdot 10^{-3} \, V$ and $4.6 \cdot 10^{-2}$ respectively but, as it will be shown in the following subsection, the phase of the input signal is not tracked accurately due to the average error.

In case of four decomposition levels ($L = 4$, in Fig. 5), the most suitable mother wavelet is *Haar* applying $GA_4 = 43$. The obtained cumulative average errors after each transient of the grid voltage are $1.1 \cdot 10^{-3} \, V$ and $2.0 \cdot 10^{-3}$ respectively. The measured ripples are $0.14 \, V$ and $0.16 \, V$ respectively. In comparison to the obtained results for $L = 3$, in this case ($L = 4$) the cumulative error after the grid frequency transient is reduced to 38%. The comparisson of the measured ripples using $L = 3$ and $L = 4$ shows that, after the first transient, $L = 4$ with *Haar* wavelets results on better results. The worst results in case of $L = 4$ are obtained
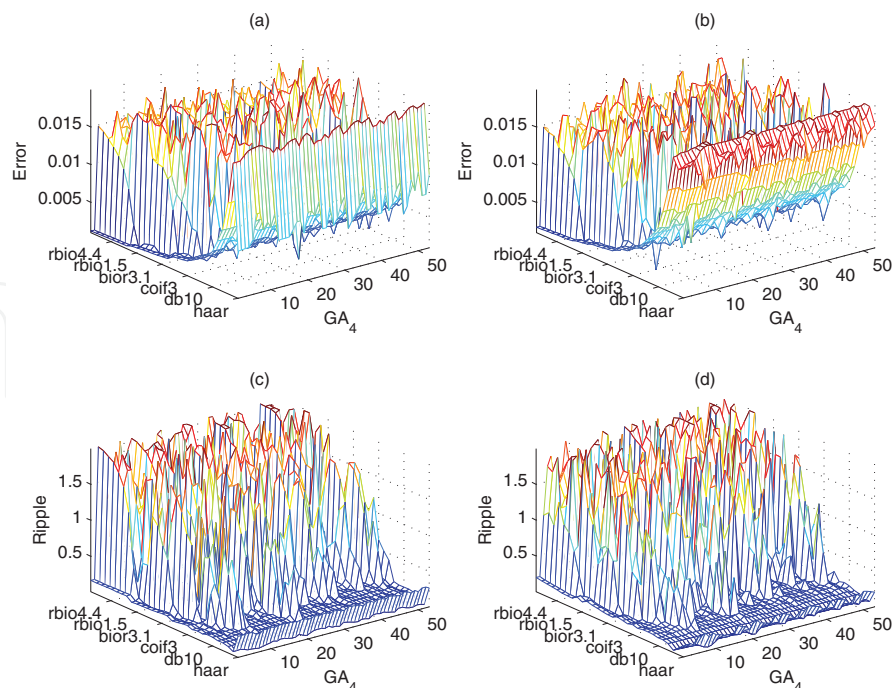
Fig. 5. L=4. a) Magnitude of the WPLL average error after the voltage amplitude step, b) magnitude of the WPLL average error after the fundamental grid frequency step, c) ripple of the WPLL error after the voltage amplitude step and d) ripple of the WPLL error after the voltage amplitude step.

by employing *Coif□et 5* as mother wavelet with $GA_4 = 21$. The obtained cumulative average errors are $2.0 \cdot 10^{-2}$ V and $8.6 \cdot 10^{-3}$ V while the measured ripples reach $1.1 \cdot 10^{-2}$ V and 1.5 V.

From Fig. 6, again *Haar* wavelets, in this case with $GA_5 = 29$, result on the best tracking of the applied grid voltage. The measured cumulative average errors were $8.1 \cdot 10^{-4}$ V and $2.6 \cdot 10^{-3}$ V after the amplitude and frequency steps respectively while, in case of the error ripple, the measured values were 0.14 V and 0.12 V. Comparing these results to the ones obtained in case of $L = 4$, the cumulative average error decreases after the amplitude step of the grid voltage due to the added fifth decomposition level. The worst results at $L = 5$ are obtained for *symlet 8*, where the cumulative average errors after the transients are $2 \cdot 10^{.2}$ V and $1.7 \cdot 10^{-2}$ V. The measured error ripples are $2.4 \cdot 10^{-2}$ and 0.16 V.

Again in case of $L = 6$ (Fig. 7), *Haar* wavelets with $GA_6 = 22$ allow the best tracking performance to be reached. The measured cumulative average errors in this case were $6.4 \cdot 10^{-4}$ V and $9.3 \cdot 10^{-4}$ V corresponding to amplitude and frequency transients respectively, which improves the obtained results in case of $L = 5$. The measured error ripples were 0.16 V and 0.22 V. The worst results were obtained in case of the mother wavelet *Biorthonormal 4.4*, with cumulative average errors equal to $2.0 \cdot 10^{-2}$ V and 1.6^{-2} V. The error ripple reached 0.02 V and 0.67 V for each grid voltage transient.

The evolution of the frequency measurement obtained by means of the WPLL in case of $L = 3$, *Daubechies 7*, $GA_3 = 39$ and $GD_3 = 30$ is shown in Fig. 8.a where the response time of the WPLL is 305 ms. Response times with *Haar* wavelet and four ($GA_4 = 43$, $GD_4 = 18.5$) and five ($GA_5 = 29$, $GD_5 = 4.5$ and $GD_4 = 3$) decomposition levels are shown in Fig. 8.b and 8.c. In these cases the measured response times are 64 ms and 150 ms corresponding to $L = 4$ and
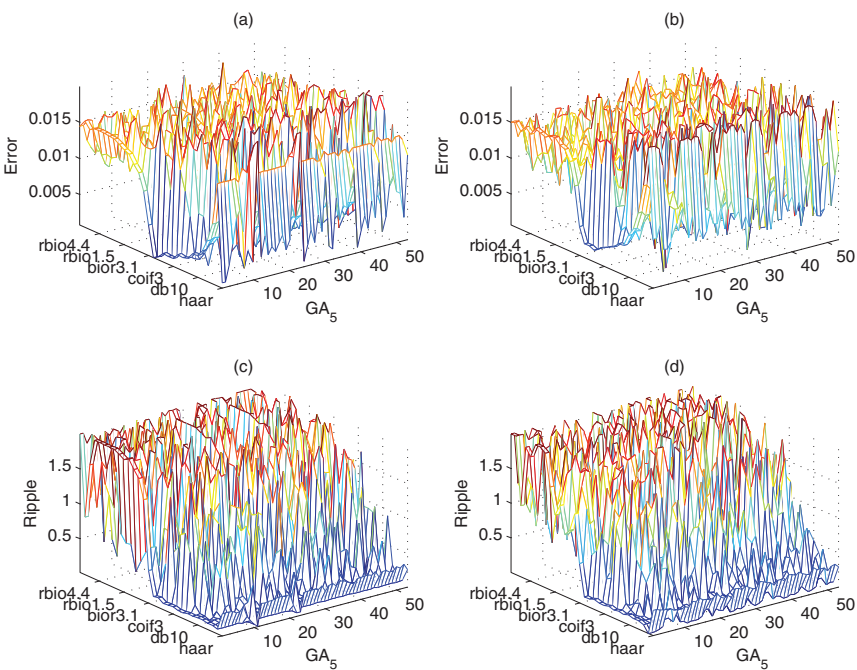
Fig. 6. L=5. a) Magnitude of the WPLL average error after the voltage amplitude step, b) magnitude of the WPLL average error after the fundamental grid frequency step, c) ripple of the WPLL error after the voltage amplitude step and d) ripple of the WPLL error after the voltage amplitude step.
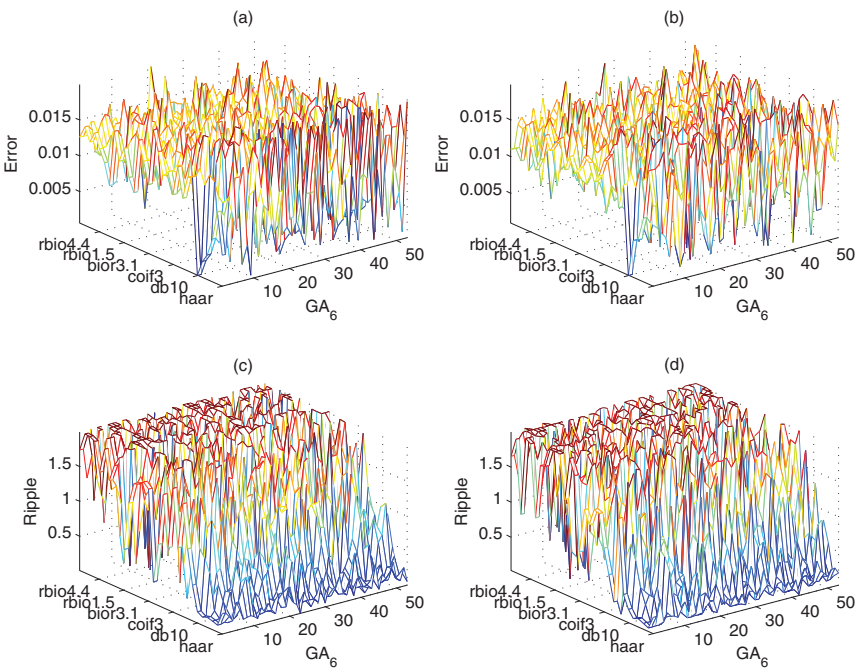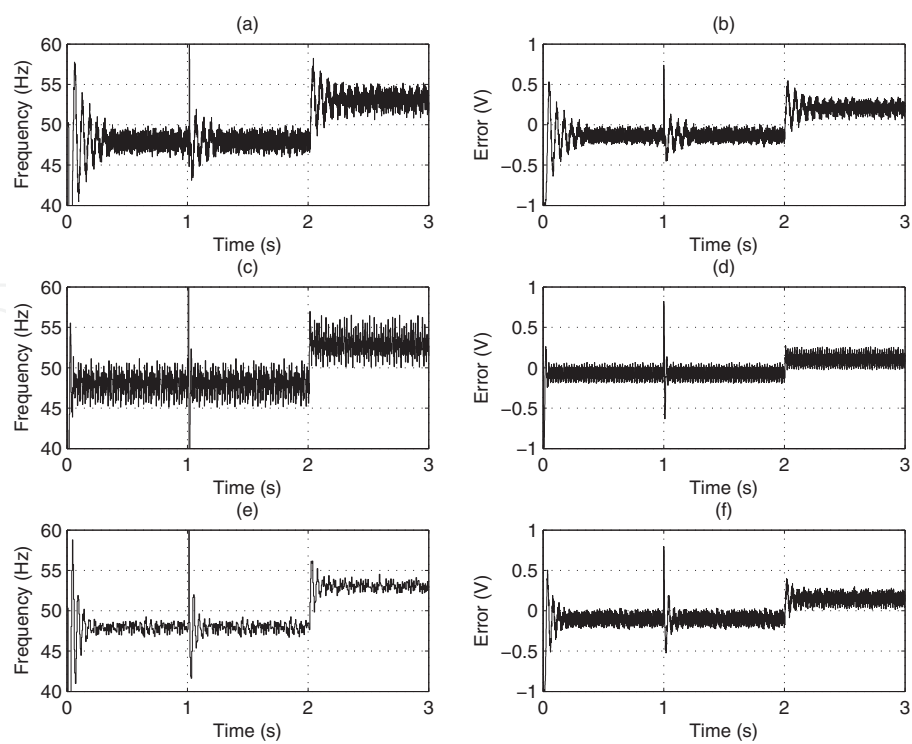

Fig. 7. L=6. a) Magnitude of the WPLL average error after the voltage amplitude step, b) magnitude of the WPLL average error after the fundamental grid frequency step, c) ripple of the WPLL error after the voltage amplitude step and d) ripple of the WPLL error after the voltage amplitude step.

Fig. 8. Time response of the WPLL. a) Frequency measurement with $L = 3$, b) WPLL error with with $L = 3$, c) Frequency measurement with $L = 4$, d) WPLL error with with $L = 4$, e) Frequency measurement with $L = 5$ and f) WPLL error with with $L = 5$.

$L = 5$. In despite of a higher number of decomposition levels, the response time of *Daubechies 7* is the longest one due to the filter length. *Haar* wavelets result on simple filter banks with low response times. Moreover, from Fig. 8.e, the WPLL performance improves by selecting more decomposition levels which results on less frequency ripple.

The WPLL outputs, considering *Daubechies 7* ($L = 3$) and *Haar* ($L = 4$ and $L = 5$), for control purposes of the grid-connected power converter can be compared by means of Fig. 9, where
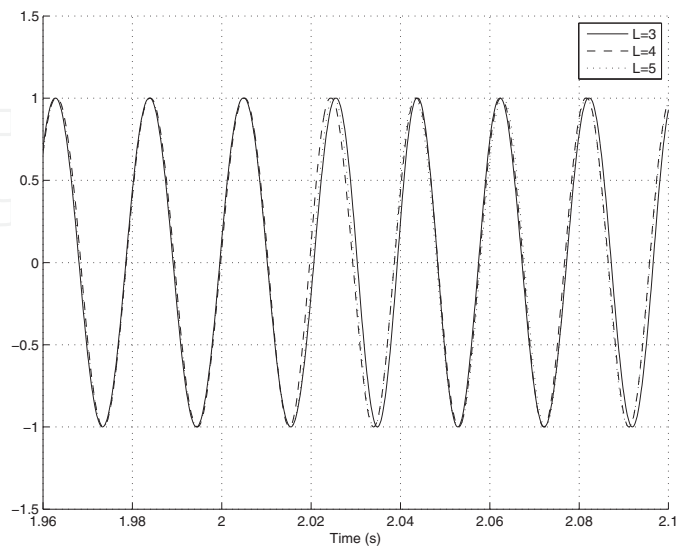

Fig. 9. Time response of the WPLL after the frequency step, at 2 s, from 47.5 Hz to 52.5 Hz.

the time response of the PLL after the frequency transient of the grid voltage (at $t = 2\ s$) is shown.

5.2 Control of a dc motor

The proposed synchronization subsystem has been tested in simulation as a part of the whole controller in case of a grid-connected power converter feeding a dc motor. The employed MatLab/Simulink simulation model, including the power stage, the converter controller and the measurement, is depicted in Fig. 10.
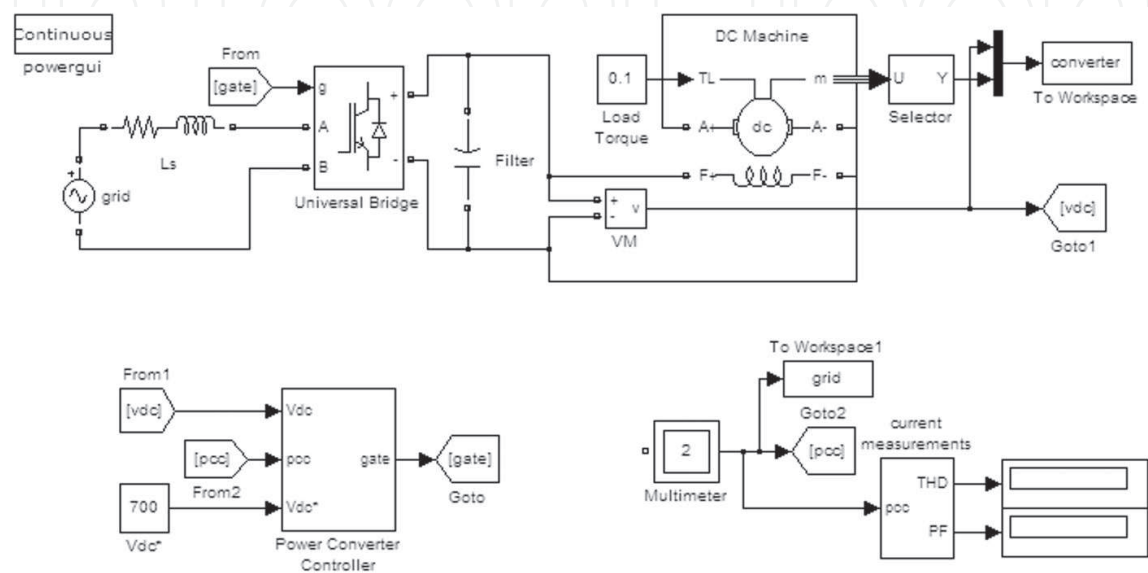
Fig. 10. MatLab/Simulink model of a dc motor controlled by means of a grid-connected power converter. Top: power stage, including the electrical grid, the power converter and the dc machine. Bottom: the controller of the power converter and measurement blocks.

The power stage includes a pure sinusoidal waveform with $230\sqrt{2}\ V$ amplitude and $50\ Hz$ frequency as grid voltage. The grid impedance and the inverter side inductance have been modeled as a series RL with values $0.4\ \Omega$ and $2.5\ mH$. The IGBT+Diode H-bridge is modeled by means of the *Universal Bridge* block of the SimPowerSystems Blockset. The dc filtering stage consist of one $550\ \mu F$ capacitor and it is connected to the dc motor windings, which are connected in series. The dc machine is modeled as a separately excited dc machine by means of the *DC Machine* block. The measured variables in this model are, at the dc motor side, the motor speed, the output voltage of the power converter (across the dc capacitor) and the output current (flowing through the dc motor), at the electrical grid side, the grid voltage and line current waveforms are also measured.

The inner structure of the employed controller is shown in Fig. 11. The power signals employed for control purposes (voltage across the dc capacitor, grid voltage and line current) are filtered out in order to avoid the aliasing due to the sampling process. The *PLL* block generates a sinusoidal signal, with unitary amplitude, which is employed to evaluate the reference current (applied to port *iGrid** in *current controller*). The proportional-integral (PI) block with $K_p = K_i = 0.4$, employed in case of the SPLL-based model, evaluates the amplitude of this reference current in order to maintain the dc bus voltage at the reference value, in this case $450\ V$. In order to compare the obatined results, the same reference voltage is employed in case of the WPLL-based model, where the *Haar* wavelet with five decomposition levels, that
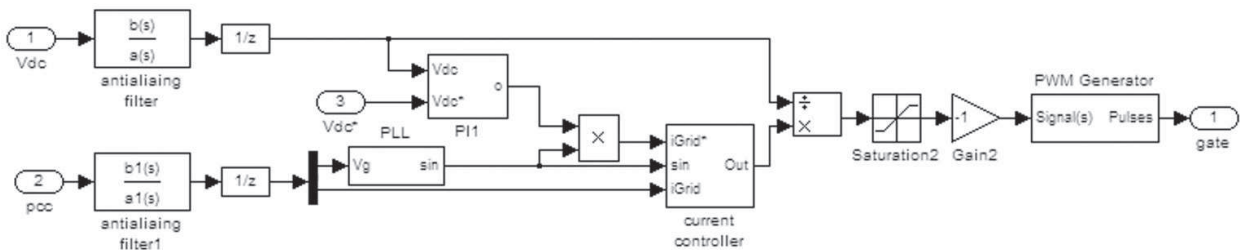
Fig. 11. Structure of the analyzed converter controller.

was analyzed in the previous sections, is applied. The current controller is implemented as a proportional-resonant controller and, in this case, three resonant blocks have been employed at frequencies $\omega_1 = 50\ Hz$, $\omega_3 = 150\ Hz$ and $\omega_3 = 250\ Hz$. The gains of the controller are $K_p = 7$ and $K_1 = K_3 = K_5 = 200$. After the control action, in order to obtain the switching pattern, the output of the current controller must be divided by the measured dc capacitor voltage. Then, the gate pulses of the H-bridge are generated by the block *PWM Generator*, which applies a triangular carrier signal whose frequency matches the sampling frequency, $f_s = 6.4\ kHz$.

The obtained results corresponding to the dc voltage, in case of both the conventional PLL and the WPLL, are shown in Fig. 12.a. As it can be seen, the WPLL subsystem results on an
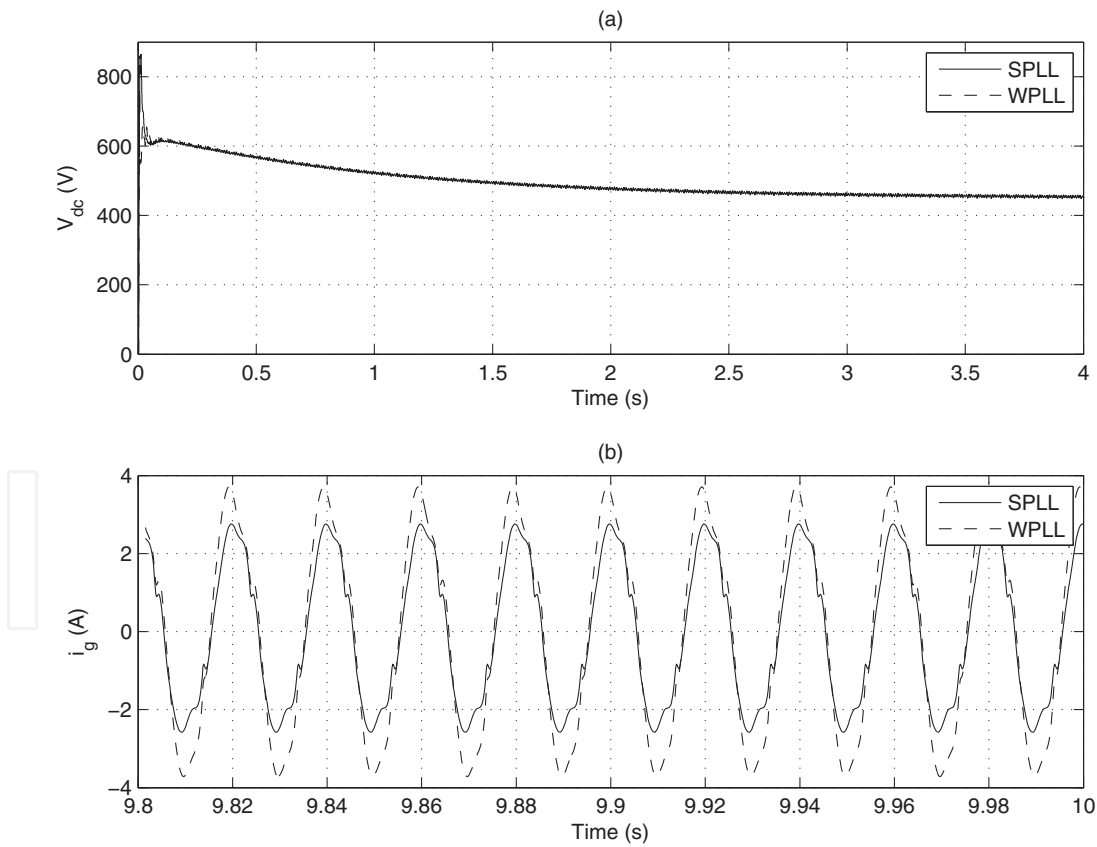

Fig. 12. Structure of the analyzed converter controller.

smoother dc voltage during the motor starting while the conventional SPLL subsystem, based on a PI controller, results on a $863\ V$ transient, which could damage the power converter and the motor windings in case of no protection. The response times in both cases, after the

starting transient, are 3.72 *s*. This is due to the fact that reference current amplitude is obtained, in both cases, by applying the same PI controller. The current line waveforms, once the dc motor reaches the steady state in both models (with the conventional SPLL and the WPLL), are shown in Fig. 12.b. The measured current THDs are 0.67% and 0.55% corresponding to the conventional SPLL and the proposedl WPLL.

6. Conclusions

This book chapter presents an application of wavelets in grid-connected power converters. The proposed approach allows wavelet-based software phase locked loops (SPLLs) to be developed and implemented, replacing the proportional-integral controller in conventional SPLLs. The proposed approach results on a more flexible synchronization subsystem whose characteristics can be adjusted depending on the electrical grid disturbances. Simulation results, comparing the performance of the conventional SPLL and the wavelet-based proposed one, are given in case of a grid-connected power converter feeding a dc motor.

7. References

Bose, B. K. (2006). *Power electronics and motor drives : advances and trends*, Academic Press.

Bose, B. K. (2009). The past, present, and future of power electronics, *IEEE Industrial Electronics Magazine* 3(2): 7–11,14.

Bueno, E. J., Cobreces, S., Rodriguez, F. J., Hernandez, A. & Espinosa, F. (2008). Design of a back-to-back npc converter interface for wind turbines with squirrel-cage induction generator, *IEEE Transactions on Energy Conversion* 23(3): 932–945.

Bueno, E. J., Hernandez, A., Rodriguez, F. J., Giron, C., Mateos, R. & Cobreces, S. (2009). A dsp- and fpga-based industrial control with high-speed communication interfaces for grid converters applied to distributed power generation systems, *IEEE Transactions on Industrial Electronics* 56(3): 654–669.

Carrasco, J. M., Franquelo, L. G., Bialasiewicz, J. T., Galvan, E., Guisado, R. C. P., Prats, M. A. M., Leon, J. I. & Moreno-Alfonso, N. (2006). Power-electronic systems for the grid integration of renewable energy sources: A survey, *IEEE Transactions on Industrial Electronics* 53(4): 1002–1016.

Castro, R. M. & Diaz, H. N. (2002). An overview of wavelet transform application in power systems, 14th *Power Systems Computation Conference*, pp. 6.1–6.9.

Chaari, O., Meunier, M. & Brouaye, F. (1996). Wavelets: a new tool for the resonant grounded power distribution systems relaying, *IEEE Transactions on Power Delivery* 11(3): 1301–1308.

Dannehl, J., Fuchs, F. W. & Thϕgersen, P. B. (2010). Pi state space current control of grid-connected pwm converters with lcl filters, *IEEE Transactions on Power Electronics* 25(9): 2320–2330.

De Mango, F., Liserre, M. & D'Aquila, A. (2006). Overview of anti-islanding algorithms for pv systems. part ii: Activemethods, *12th International Power Electronics and Motion Control Conference, EPE-PEMC 2006*, pp. 1884–1889.

De Mango, F., Liserre, M., D'Aquila, A. & Pigazo, A. (2006). Overview of anti-islanding algorithms for pv systems. part i: Passive methods, *12th International Power Electronics and Motion Control Conference, EPE-PEMC 2006*, pp. 1878–1883.

Dinkhauser, V. & Fuchs, F. W. (2008). Rotor turn-to-turn faults of doubly-fed induction generators in wind energy plants - modelling, simulation and detection, *13th International Power Electronics and Motion Control Conference*, pp. 1819–1826.

Driesen, J. & Belmans, R. (2002). Active power filter control algorithms using wavelet-based power definitions, *10th International Conference on Harmonics and Quality of Power*, Vol. 2, pp. 466–471.

El-Amawy, A. A. & Mirbod, A. (1988). An efficient software-controlled pll for low-frequency applications, *IEEE Transactions on Industrial Electronics* 35(2): 341 – 344.

Eren, L. & Devaney, M. J. (2001). Motor bearing damage via wavelet analysis of starting current transient, *Proc. of the 18th IEEE Instrumentation and Measurement Technology Conference*, Vol. 3, pp. 1797–1800.

Erickson, R. W. & Maksimovic, D. (2001). *Fundamentals of power electronics*, Kluwer.

Freijedo, F. D., Doval-Gandoy, J., Lopez, O. & Acha, E. (2009). Tuning of phase-locked loops for power converters under distorted utility conditions, *IEEE Transactions on Industry Applications* 45(6): 2039–2047.

Gabe, I. J., Montagner, V. F. & Pinheiro, H. (2009). Design and implementation of a robust current controller for vsi connected to the grid through an lcl filter, *IEEE Transactions on Power Electronics* 24(6): 1444–1452.

Gandelli, A., Monti, A., Ponci, F. & Santi, E. (2001). Power converter control design based on haar analysis, *IEEE 32nd Annual Power Electronics Specialists Conference, PESC 2001.*, Vol. 3, pp. 1742–1746.

Gandelli, A., Monti, A., Santi, E. & Ponci, F. (2002). Extending haar domain analysis to dc/ac converters, *IEEE Annual Power Electronics Specialists Conference*, Vol. 4, pp. 1717–1721.

González, D., Bialasiewicz, J. T., Balcells, J. & Gago, J. (2008). Wavelet-based performance evaluation of power converters operating with modulated switching frequency, *IEEE Transactions on Industrial Electronics* 55(8): 3167–3176.

Guerrero, J. M., de Vicuna, L. G., Matas, J., Castilla, M. & Miret, J. (2004). A wireless controller to enhance dynamic performance of parallel inverters in distributed generation systems, *IEEE Transactions on Power Electronics* 19(5): 1205–1213.

Hamid, E. Y. & Kawasaki, Z. L. (2001). Wavelet packet transform for rms values and power measurements, *IEEE Power Engineering Review* 21(9): 49–51.

Heydt, G. & Galli, A. (1997). Transient power quality problems analyzed using wavelets, *IEEE Transactions on Power Delivery* 12(2): 908–915.

Ho, C. N.-M., Cheung, V. S. P. & Chung, H. S.-H. (2009). Constant-frequency hysteresis current control of grid-connected vsi without bandwidth control, *IEEE Transactions on Power Electronics* 24(11): 2484–2495.

Holmes, D. G. & Lipo, T. A. (2003). *Pulse Width Modulation for Power Converters: Principles and Practice*, Power, Energy & Industry Applications, 1 edn, Wiley-IEEE Press.

Hsu, C.-F., Lee, T.-T. & Wang, S.-L. (2008). Fpga-based adaptive wavelet neurocontroller design for dc-dc converter, *Proc. of the 7th International Conference on Machine Learning and Cybernetics (ICMLC)*, Vol. 7, pp. 3833–3838.

Huang, C. & Yang, H. T. (2001). Evolving wavelet-based netors for short-term load forecasting, *IEE Proceedings - Generation, Transmission and Distribution* 148(3): 222–228.

Iwaszkiewicz, A. J. & Perz, B. J. (2007). A novel approach to control of multilevel converter using wavelets transform, *International Conference on Renewable Energies and Power Quality*.

Kazmierkowski, M. P., Krishnan, R. & Blaabjerg, F. (eds) (2002). *Control in power electronics : selected problems*, Academic Press.

Knezevic, J., Katic, V. & Graovac, D. (2000). Transient analysis of ac/dc converters input waveforms using wavelet, *Proceedings of the Mediterranean Electrotechnical Conference*, Vol. 3, pp. 1193–1196.

Koizumi, H., Mizuno, T., Kaito, T., Noda, Y., Goshima, N., Kawasaki, M., Nagasaka, K. & Kurokawa, K. (2006). A novel microcontroller for grid-connected photovoltaic systems, *IEEE Transactions on Industrial Electronics* 53(6): 1889–1897.

Kojabadi, H. M., Yu, B., Gadoura, I. A., Chang, L. & Ghribi, M. (2006). A novel dsp-based current-controlled pwm strategy for single phase grid connected inverters, *IEEE Transactions on Power Electronics* 21(4): 985–993.

Liserre, M., Sauter, T. & Hung, J. Y. (2010). Future energy systems: Integrating renewable energy sources into the smart power grid through industrial electronics, *IEEE Industrial Electronics Magazine* 4(1): 18–37.

Liserre, M., Teodorescu, R. & Blaabjerg, F. (2006). Multiple harmonics control for three-phase grid converter systems with the use of pi-res current controller in a rotating frame, *IEEE Transactions on Power Electronics* 21(3): 836–841.

McGrath, B. P., Holmes, D. G. & Galloway, J. J. H. (2005). Power converter line synchronization using a discrete fourier transform (dft) based on a variable sample rate, *IEEE Transactions on Power Electronics* 20(4): 877–884.

Mercorelli, P., Kubasiak, N. & Liu, S. (2004). Model predictive control of an electromagnetic actuator fed by multilevel pwm inverter, *IEEE International Symposium on Industrial Electronics*, Vol. 1, pp. 531–535.

Mohamed, Y. A.-R. & El-Saadany, E. F. (2008). Adaptive discrete-time grid-voltage sensorless interfacing scheme for grid-connected dg-inverters based on neural-network identification and deadbeat current regulation, *IEEE Transactions on Power Electronics* 23(1): 308–321.

Mohan, N., Undeland, T. M. & Robbins, W. P. (2003). *Power electronics : converters, applications and design*, John Wiley & Sons.

Moreno, V. M., Liserre, M., Pigazo, A. & Dell'Aquila, A. (2007). A comparative analysis of real-time algorithms for power signal decomposition in multiple synchronous reference frames, *IEEE Transactions on Power Electronics* 22(4): 1280–1289.

Parvez, S. & Gao, Z. (2005). A wavelet-based multiresolution pid controller, *IEEE Transactions on Industry Applications* 41(2): 537–543.

Pham, V. L. & Wong, K. P. (1999). Wavelet-transform-based algorithm for harmonic analysis of power system waveforms, *IEE Proceedings - Generation and Distribution* 146(3): 249–254.

Pham, V. L., Wong, K. P. & Arrillaga, J. (2000). Sub-harmonics state estimation in power system, *IEEE Power Engineering Society Winter Meeting*, Vol. 2, pp. 1168–1173.

Pigazo, A., Liserre, M., Mastromauro, R. A., Moreno, V. M. & Dell'Aquila, A. (2009). Wavelet-based islanding detection in grid-connected pv systems, *IEEE Transactions on Industrial Electronics* 56(11): 4445–4455.

Pigazo, A., Moreno, V. M., Liserre, M. & Dell'Aquila, A. (2007). Wavelet-based islanding detection algorithm for single-phase photovoltaic (pv) distributed generation systems, *IEEE International Symposium on Industrial Electronics*, pp. 2409–2413.

Ponci, F., Santi, E. & Monti, A. (2009). Discrete-time multi-resolution modeling of switching power converters using wavelets, *Simulation* 85(2): 69–88.

Ribeiro, P. F. (1994). Wavelet transform: an advanced tool for analysing non-stationary harmonic distortion in power system, *Proc. of the IEEE International Conference on Harmonics in Power Systems*.

Robertson, D., Camps, O. & Mayer, J. (1994). Wavelets and power system transients, *SPIE International Symposium on Optical Engineering in Aerospace Sensing*, pp. 474–487.

Saleh, S. A. & Rahman, M. A. (2009). Performance testing of a single-phase voltage-source wavelet modulated ac-dc converter, *Canadian Conference on Electrical and Computer Engineering, CCECE '09*, pp. 1049–1054.

Shim, I., Soragan, J. J., Siew, W. H., Sludden, K. & Gale, P. F. (2000). Robust partial discharge measurement in mv cable networks using discrete wavelet transforms, *IEEE Power Engineering Society Winter Meeting*, Vol. 1, pp. 718–723.

Solanki, M., Song, Y. H., Potts, S. & Perks, A. (2001). Transient protection of transmission lines using wavelet transform, *IEEE 7th International Conference on Developments in Power System Protection*, pp. 299–302.

Sumner, M., Abusorrah, A., Thomas, D. & Zanchetta, P. (2006). Improved power quality control and intelligent protection for grid connected power electronic converters, using real time parameter estimation, *IEEE Industry Applications Society Annual Meeting*, Vol. 4, pp. 1709–1715.

Teng, L.-T., Lin, F.-J., Chiang, H.-C. & Lin, J.-W. (2009). Recurrent wavelet neural network controller with improved particle swarm optimisation for induction generator system, *IET Electric Power Applications* 3(2): 147–159.

Ullah, N., Bhattacharya, K. & Thiringer, T. (2009). Wind farms as reactive power ancillary service providersŮtechnical and economic issues, *IEEE Transactions on Energy Conversion* 24(3): 661–672.

Vainio, O. & Ovaska, S. (1995). Noise reduction in zero crossing detection by predictive digital filtering, *IEEE Transactions on Industrial Electronics* 42(1): 58–62.

Valiviita, S. (1999). Zero-crossing detection of distorted line voltages using 1-b measurements, *IEEE Transactions on Industrial Electronics* 46(5): 917–922.

Weiss, G., Zhong, Q.-C., Green, T. C. & Liang, J. (2004). h^{∞} repetitive control of dc-ac converters in microgrids, *IEEE Transactions on Power Electronics* 19(1): 319–230.

Wilkinson, W. A. & Cox, M. D. (1996). Discrete wavelet analysis of power system transient, *IEEE Transactions on Power Systems* 11(4): 2018–2044.

Yao, S. J., Song, Y. H., Zhan, L. Z. & Cheng, X. Y. (2000). Wavelet transform and neural networks for short-term electrical forecasting, *Energy Conversion and Management* 41(18): 1975–1988.

Zhen, R., Qungu, H., Lin, G. & Weniying, H. (2000). A new method for power system frequency tracking based on trapezoid wavelet transform, *International Conference on advances in Power System Control, Operation and Management*, Vol. 2, pp. 364–369.

Discrete Wavelet Transforms - Theory and Applications

Edited by Dr. Juuso T. Olkkonen

Discrete wavelet transform (DWT) algorithms have become standard tools for discrete-time signal and image processing in several areas in research and industry. As DWT provides both frequency and location information of the analyzed signal, it is constantly used to solve and treat more and more advanced problems. The present book: Discrete Wavelet Transforms: Theory and Applications describes the latest progress in DWT analysis in non-stationary signal processing, multi-scale image enhancement as well as in biomedical and industrial applications. Each book chapter is a separate entity providing examples both the theory and applications. The book comprises of tutorial and advanced material. It is intended to be a reference text for graduate students and researchers to obtain in-depth knowledge in specific applications.

How to reference

In order to correctly reference this scholarly work, feel free to copy and paste the following:

Alberto Pigazo and Víctor M. Moreno (2011). Discrete Wavelet Transforms for Synchronization of Power Converters Connected to Electrical Grids, Discrete Wavelet Transforms - Theory and Applications, Dr. Juuso T. Olkkonen (Ed.), ISBN: 978-953-307-185-5, InTech, Available from:

http://www.intechopen.com/books/discrete-wavelet-transforms-theory-and-applications/discrete-wavelet-transforms-for-synchronization-of-power-converters-connected-to-electrical-grids

INTECH
open science | open minds